Possible band-structure shapes of quasi-one-dimensional solids

Ivan Božović*
Department of Physics, University of California, Berkeley, California 94720
(Received 2 August 1983; revised manuscript received 5 January 1984)

The well-known restrictions on the possible shapes of electron energy bands arising from one-dimensional (1D) periodic potentials do not apply to chainlike physical systems such as polymers or molecular stacks, which are three dimensional objects periodic along a line. For such quasi-one-dimensional (Q1D) crystals, bands can be nondegenerate, but they may also contact one another at the center and/or at the boundaries of the Brillouin zone (BZ), cross at a general k point, or be degenerate throughout the BZ, so that a variety of topologically inequivalent shapes can be formed. These shapes are essentially determined by the spatial symmetry of the Q1D object considered, i.e., by its line group. A complete classification has been worked out, and for every possible Q1D crystal structure the corresponding band shapes are specified. The method focuses on the quantum numbers having clear physical meaning (quasimomentum, quasi angular momentum, etc.); elaborate group-theoretical parlance is avoided. Furthermore, it is studied how this complexity of band shapes which may occur in Q1D crystals affects some predicted physical properties—optical-absorption spectra and vibronic coupling, in particular. First, each singularity of the density-of-states function bears definite symmetry labels, and many direct interband transitions in polymers are forbidden by the line-group selection rules. Next, in the case of electronic degeneracy, many different types of vibronic instabilities are possible. Depending on the line group, the band shapes, and the quantum numbers of the electronic states involved, the active phonons may be longitudinal or transversal, acoustic or optical, single or degenerate, displacive or distortive, etc.; also, various types of symmetry breaking can occur. Finally, applicability to other quasi particles (phonons, etc.) and to solids of higher dimensionality is pointed out.

I. INTRODUCTION

The conductivity of several polymers can be varied over broad ranges upon doping—by as much as 20 orders of magnitude in the case of poly(*p*-phenylene). This and other interesting phenomena—superconductivity in organic materials, charge- and spin-density waves, solitons—motivated extensive studies of electronic properties of polymers and quasi-one-dimensional (Q1D) solids.[1] Frequently, in such studies one calculates the band structure of an isolated periodic chain of atomic clusters. Any irregularities, finite length effects, and the interchain interaction are disregarded at this level of approximation. For brevity, in this paper we refer to such model chains as "polymers" and to the clusters as "monomers."

Band structures have been calculated for a number of polymers, but what is still lacking are some general statements about possible band shapes, cohering, crossings, location of the extrema, etc. This paper attempts to fill in this gap with the following motivation. Computations in quantum theory of polymers are often very elaborate, and errors that are difficult to detect are possible as evidenced by frequent reassessments of incorrect Hamiltonian truncations or incorrect band interpolations (cf. Ref. 2 for a discussion of "band indexing difficulties"). It might appear as if an error of a few percent is irrelevant here in view of the approximations already made, but if an artificial gap is opened in the vicinity of the Fermi level, the density of states (DOS) can be changed considerably in this most sensitive region, and a completely wrong prediction of properties such as infrared absorption or conductivity may result. The essential qualitative features of band structures should therefore be assured. In addition, such a qualitative account brings in some conceptual insight, and finally, systematic listing of all the possible band shapes may show that some interesting special cases have escaped our attention yet.

The major source of inspiration for this work were the classical studies of Van Hove singularities in three-dimensional (3D) and two-dimensional (2D) crystals by Van Hove,[3] Phillips,[3] and others;[3] they had considered the one-dimensional (1D) case trivial. Indeed, a strictly 1D periodic potential $V(z)\equiv V(z+a)$ gives rise to energy bands which do not intersect and which have extrema only at the center and at the edges of the Brillouin zone (BZ). However, a polymer is described by a potential $V(x,y,z)$ which is *not* 1D, although it is still periodic in one direction only, $V(x,y,z)\equiv V(x,y,z+a)$. It is rather *quasi-one-dimensional,* as the lateral extension of a polymer is typically rather small; still, the above conclusions about the band structure need not be valid for all polymers.[4] On the contrary, we have found a surprising richness of band shapes; the characteristic ones are sketched in Fig. 1, where we also introduce some descriptive nomenclature for further reference. [Normally, we plot only one-half of the BZ, assuming the bands to be symmetric with respect to the $k=0$ axis—the effective one-electron Hamiltonians utilized in the quantum theory of polymers are usually invariant with respect to the time reversal θ, and hence $\{\epsilon_\lambda(k),\ \lambda=1,2,\ldots\}\equiv\{\epsilon_\lambda(-k),\ \lambda=1,2,\ldots\}$.

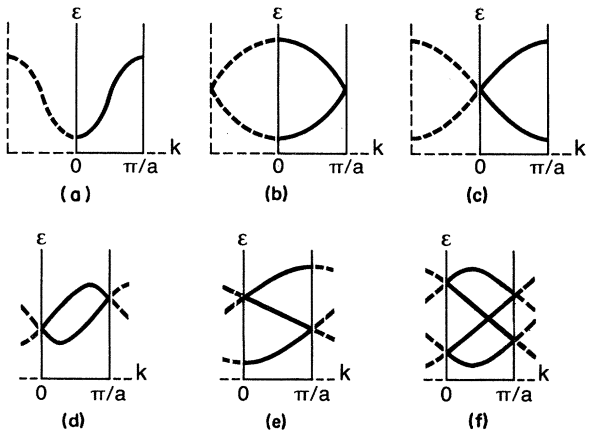

FIG. 1. Some band shapes possible in polymers: (a) line, (b) semiloop, (c) semicross, (d) loop, (e) S shape, and (f) butterfly.

More general Hamiltonians are discussed briefly in Sec. VII.]

The band structure of the polymer depends on its chemical and spatial structure, and hence the next step is to look for the correspondence between a particular band shape and the related structural features. For this purpose an appropriate classification of polymer structures is needed; it turns out that the decisive factor is the symmetry of the polymer, described technically by its *line group*. Hence, in this work we use the line-group theoretical results to address the above question; however, we avoid group-theoretical parlance and express the results in terms of a few quantum numbers having clear physical meaning (quasimomentum, quasi angular momentum, etc).

This paper is organized as follows. In Sec. II it is outlined how we determine the band shapes utilizing the information about the symmetry of the polymer, and the possible symmetry elements are described. Each possible symmetry group is then discussed separately in Secs. III–V. The rotation symmetry is dealt with first, in Sec. III, where the quasi angular momentum is also introduced, its behavior under various operations is analyzed, and the conservation law it obeys is specified. The occurrence of loops and twofold-degenerate bands is illustrated by means of simple model example, and it is also shown how symmetry reduction, caused by a perturbation or by a structural change, influences the DOS peak structure and the selection rules. In Sec. IV helical polymers are considered, and in Sec. V glide planes are dealt with; the appearance of semicrosses, single and double semiloops, "butterflies," and other more complex band shapes is documented. Symmetry-generated quantum numbers, especially the quasi angular momentum, remain the main tool in the analysis. In Sec. VI these results are applied to investigate vibronic instabilities caused by electronic degeneracy in Q1D solids. Finally, in Sec. VII the conclusions are summarized, stressing that although the number of possible inequivalent band shapes is unlimited, all of them can be reduced to only a few simple ones in the Jones-zone (JZ) scheme. Applicability of the results of this paper for solids of higher dimensionality and quasiparticles other than electrons is also pointed out.

II. METHOD FOR DETERMINING BAND SHAPES

Let $\epsilon_\lambda(k)$, $\lambda=1,2,\ldots$, $-\pi/a<k\leq\pi/a$, denote the energy bands of a polymer with the symmetry group $\underline{L}$. Our conclusions about the band shapes are based on a few observations, which can be vaguely stated as follows: (i) Each $\epsilon_\lambda(k)$ is a continuous function of k, (ii) $\underline{L}$ determines the degeneracies of $\epsilon_\lambda(k)$, and (iii) some information about the zero-slope points can be inferred from (i) and (ii). Indeed, a polymer is invariant with respect to translations that form a discrete set, so that k also assumes only a discrete set of values from the interval $(-\pi/a, \pi/a]$. Furthermore, the Born–von Kármán periodic boundary condition is usually imposed, which makes both sets finite. However, if that period is sufficiently large to contain many elementary cells, the set of allowed values of k is sufficiently dense to enable one to speak about quasicontinuity of the bands $\epsilon_\lambda(k)$. (See, e.g., the discussion of $\vec{k}\cdot\vec{p}$ perturbation expansion given in Ref. 5.)

The symmetry groups of polymers are the *line groups*,[6] and their role in polymer physics parallels that of the point groups in molecular physics or that of the crystallographic space groups in solid-state physics. An elementary description of the line groups is given below. Knowing the irreducible representations[7] (irreps of the line groups, one can label the energy levels and the eigenstates, determine the degeneracies, construct symmetry-adapted bases, and derive selection rules for various processes.[8] The band connectivities can be inferred from the so-called *compatibility relations*;[9] here, we report the first derivation of such relations, for all the irreps of all the line groups. Notice that these relations must be satisfied if the effective one-electron Hamiltonian H commutes with the line group $\underline{L}$ of the polymer under study. (However, an unrestricted Hartree-Fock solution can, in general,[5] generate a Fock operator of some lower symmetry $\underline{L}'$.)

Apart from the systematic degeneracies, some additional band crossings may be an unavoidable feature of a particular connectivity scheme; an example is given in Fig. 1(f). Occurrence of such crossings can be predicted, but their exact location cannot be determined from symmetry arguments alone.

Finally, our conclusions about the zero-slope point are based on the following facts. The band structure must be symmetric with respect to the $k=0,\pm\pi/a,\ldots$, vertical axes (because of the translational periodicity of the polymer and the time-reversal invariance), but one particular $\epsilon(k)$ line need not have this symmetry if we connect it at the BZ edges in such a way that it remains smooth throughout the extended zone. A single line must traverse vertical symmetry axes at a right angle, but if two lines cross at $k=0$ [as in Fig. 1(c)] or at $k=\pi/a$ [Fig. 1(b)], their slopes are opposite and, in general, nonzero. Furthermore, if two lines cross at both $k=0$ and π/a to form a loop as in Fig. 1(d), there must be a minimum and a maximum somewhere inside the interval $(0, \pi/a)$. The same is true for the butterfly diagram of Fig. 1(f); in Sec.

IV B it is shown how this case can be reduced to the preceding one.

A line group $\underline{L}$ is a symmetry group of a physical object periodic along a line (for example, along the z axis). The elements of $\underline{L}$ are transformations $(R \mid t+v)$ defined by $(R \mid t+v)\vec{r}=R\vec{r}+(t+v)a\vec{e}_z$, where $t=0,\pm1,\ldots,\ 0\leq v<1$; a is the translation period, and R is a rotation, a reflection, or a rotoreflection such that it leaves the z axis invariant. Thus R can be the rotation through $2\pi/n$ around the z axis (denoted C_n), the rotation through π around the x axis (U), the reflection in the x-z plane (σ_v), the reflection in the x-y plane (σ_h), or any combination of these operations. The pure translations $(E \mid t)$ form a discrete 1D translational group $\underline{T}$, which is a subgroup of $\underline{L}$. All $(R \mid 0)$ form the point group $\underline{P}$, which can be any one of the point groups $\underline{C}_n$, $\underline{C}_{nv}$, $\underline{C}_{nh}$, $\underline{S}_{2n}$, $\underline{D}_n$, $\underline{D}_{nd}$, and $\underline{D}_{nh}$, where $n=1,2,\ldots$. $\underline{P}$ is a subgroup of $\underline{L}$ only if the latter is symmorphic, i.e., if it contains neither (intrinsic) glide planes nor (intrinsic) screw axes, so that $v=0$ in every element of $\underline{L}$. In a nonsymmorphic line group, $v\neq0$ in some elements. A rotation C_n followed by a translation by pa/n along $\vec{e}_z$ gives $(C_n \mid p/n)$, a screw axis; $(\sigma_v \mid 1/2)$ is a glide plane. We denote a line group by a Hermann-Mauguin (international crystallographic) symbol with the prefix $\underline{L}$ for the linear lattice.

In a quantum-mechanical description, one utilizes a state space V; a symmetry transformation $(R \mid t+v)$ is represented in V by a unitary operator $[R \mid t+v]$ defined by $[R \mid t+v]\Psi(\vec{r})=\Psi((R \mid t+v)^{-1}\vec{r})$. We abbreviate $[R \mid 0]$ by R. The time inversion $t\rightarrow-t$ is represented by an antiunitary operator θ, which can be simply defined here by $\theta\Psi(\vec{r})=\Psi^*(\vec{r})$. Adding θ to a line group $\underline{L}$, we extend it onto a gray line group $\underline{L}^4=\underline{L}+\theta\underline{L}$; more details can be found in Refs. 6 and 7.

The mentioned symmetry elements are all found in real physical systems (or at least in their model descriptions utilized in theoretical physics); many examples are given in Refs. 6, 10, and 11.

III. ECLIPSED STACKS: ROTATION AXES, MIRROR PLANES

In this section we consider the more simple case of the line groups which contain neither intrinsic screw axes nor intrinsic glide planes (i.e., the symmorphic line groups). An array of identical molecules, stacked in the eclipsed position, display such a symmetry; another example is a periodic linear chain of atoms. Such polymers are invariant with respect to certain rotations around the chain axis, and we begin by analyzing the effects of this symmetry on the band structure of the polymer.

A. Rotations around the chain axis

If a single molecule is invariant with respect to $\underline{C}_n$ and if it has no other symmetry, its one-electron eigenfunctions are of the form

$$\psi_m(\rho,\phi,z)=\exp(im\phi)u(\rho,\phi,z)\ , \tag{1a}$$

with

$$u(\rho,\phi-\alpha,z)\equiv u(\rho,\phi,z)\ , \tag{1b}$$

where $\alpha=2\pi/n$. The integer m is the quantum number of quasi angular momentum;[12] it has only n inequivalent values, and our standard choice is

$$m=\begin{cases}0,\pm1,\ldots,\pm(n-1)/2 & \text{for } n \text{ odd}\ , \quad (2a)\\ 0,\pm1,\ldots,\pm(n-2)/2,n/2 & \text{for } n \text{ even}\ . \quad (2b)\end{cases}$$

Notice the complete analogy between (1) and the Bloch theorem, which in our case reads

$$\psi_k(\rho,\phi,z)=\exp(ikz)u(\rho,\phi,z)\ , \tag{3a}$$

with

$$u(\rho,\phi,z-a)\equiv u(\rho,\phi,z)\ , \tag{3b}$$

where $-\pi/a<k\leq\pi/a$.

Periodic stacking of such molecules produces a polymer invariant with respect to the rotations from $\underline{C}_n$ as well as to the translations from $\underline{T}$. The line group is denoted by $\underline{L}n$, and its elements are of the form $(C_n^s \mid t)$, where $s=0,1,\ldots,n-1$, and $t=0,\pm1,\ldots$. Combining (1) and (3), we conclude that in the case of the polymer under study, the eigenfunctions are of the form

$$\psi_{km}(\rho,\phi,z)=\exp(ikz)\exp(im\phi)u(\rho,\phi,z)\ , \tag{4a}$$

with

$$u(\rho,\phi,z-a)\equiv u(\rho,\phi-\alpha,z)\equiv u(\rho,\phi,z)\ , \tag{4b}$$

where $-\pi/a<k\leq\pi/a$ and m is given by (2). For m fixed, all ψ_{km} span a subspace V_m of the state space V. These subspaces are mutually orthogonal, and one can solve the eigenproblem of H in each V_m separately. The continuity argument is still valid and each band is a (quasi) smooth function of k. (If two bands with the same quantum number m cross accidentally, the potential can always be modified slightly in such a way that the symmetry of the chain is preserved while the crossing is avoided.[13]) For a complete specification we need an additional index λ, which we choose to enumerate the bands having the same value of m in the order of ascending energies at $k=0$: $\epsilon_m^1(0)\leq\epsilon_m^2(0)\leq\cdots$. We let $\mid k,m,\lambda\rangle$ be the eigenstate of $\epsilon_m^\lambda(k)$; from (4a) and (4b) it follows that

$$[C_n^s \mid t]\mid k,m,\lambda\rangle=(\text{phase factor})\times\mid k,m,\lambda\rangle\ , \tag{5}$$

and

$$\theta\mid k,m,\lambda\rangle=\mid -k,-m,\lambda\rangle\ , \tag{6}$$

and, for $K=0,\pm2\pi/a,\pm4\pi/a,\ldots$,

$$\mid k,m,\lambda\rangle=\mid k+K,m,\lambda\rangle\ . \tag{7}$$

Of course, if at certain k there is an eigenvalue ϵ, an identical eigenvalue must be found at every $k+K$; however, the nontrivial content of the above "umklapp theorem" (7) is that the other two quantum numbers of the corresponding eigenstate must be equal also. [This implies that each $\epsilon_m^\lambda(k)$ line has a period equal to $2\pi/a$, the width of the BZ; it will be seen in Sec. IV that this is indeed not true, in general.]

Now, we are ready to discuss the coherence of bands.

Since H is real, it follows from (6) that $\epsilon^{\lambda}_{m}(k)=\epsilon^{\lambda}_{-m}(-k)$. For $k=0$ this implies that $\epsilon^{\lambda}_{m}(0)=\epsilon^{\lambda}_{-m}(0)$—at $k=0$, every "chiral" band (i.e., such that $m\neq 0$ and $n/2$) contacts another band with the opposite quasi angular momentum. Similar conclusions apply to the zone edge, since $\epsilon^{\lambda}_{m}(\pi/a)=\epsilon^{\lambda}_{-m}(\pi/a)$. A "typical" form of bands that satisfies both conditions is sketched in Fig. 2(a) for a chain of $\underline{L}n$ symmetry (with $n\geq 3$) for $m=0,\pm 1$. The $m=0$ band is single and nondegenerate; the $m=1$ band contacts the $m=-1$ band at both $k=0$ and π/a to form a closed loop. If the picture is extended to other BZ's as in Fig. 2(b), we see that the latter two bands are in fact threading and crossing at $k=0,\pm\pi/a,\pm 2\pi/a,\ldots$; the period of each band is $2\pi/a$.

The quantum numbers k and m are subject to strong selection rules. If $A_{q\mu}$ is an (irreducible tensorial) operator transforming in the manner of $|\,q,\mu\,\rangle$, one finds[5] that

$$\langle k',m',\lambda'\,|\,A_{q\mu}\,|\,k,m,\lambda\rangle=0$$

$$\text{unless } \Delta k\doteq q \text{ and } \Delta m\doteq \mu\ , \qquad (8)$$

where $\Delta k\equiv k'-k$, $\Delta m\equiv m'-m$ and where $\doteq$ means "equals up to equivalence," i.e., "equals modulo $2\pi/a$" for k and "equals modulo n" for m. Hence, both momenta are conserved in scattering processes if we include those of the perturbation.

For example, in the case of direct optical absorption, one has[8] $q\approx 0$, while μ depends on the direction of incidence and polarization: $\mu=0$ for the light polarized along the chain, while if the light beam is incident along the chain $\mu=\pm 1$ for linear polarization and $\mu=+1$ (-1) for the right (left) circular polarization.

Now, we can consider other more complicated, but logically possible connectivity schemes for the $m=1$ and the $m=-1$ bands of the eclipsed-stack polymer under study. Let A_{00} be a small change of the potential with the full symmetry of the chain; then, $\langle k,m',\lambda'\,|\,A_{00}\,|\,k,m,\lambda\rangle=0$, unless $m=m'$. Thus it is crucial whether the two bands have different or identical symmetry labels—in the first case [Fig. 3(a)] crossing is allowed, and in the second one [Fig. 3(b)] it is "avoided." The significance of splitting the "nonessential" butterfly into two separate loops is that two extra peaks emerge in the DOS function [Fig. 3(b)].

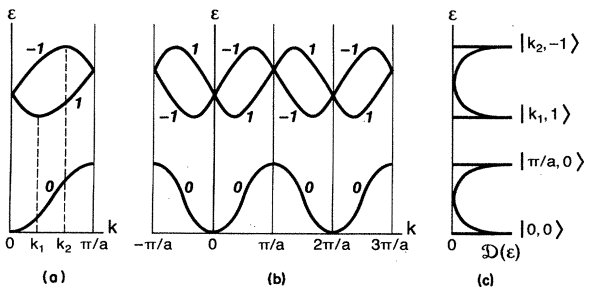

FIG. 2. Simplest possible band shapes for a polymer of $\underline{L}n$ symmetry (a) in the Brillouin zone and (b) in the extended-zone representation. The corresponding DOS peaks are sketched in (c).

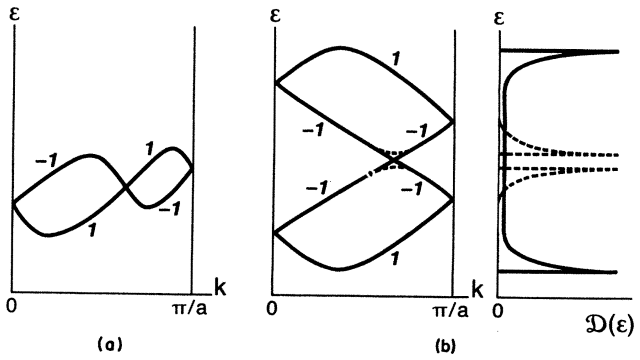

FIG. 3. More complex band shapes for a polymer of $\underline{L}n$ symmetry. (a) Allowed crossing—the intersecting bands have different quasi angular momenta. (b) Avoided crossing; butterfly opens into two loops so that two extra peaks appear in the DOS function.

B. Dihedral axes

We let U denote a rotation through π around an axis orthogonal to the main axis; if we choose the first one to coincide with the x axis, then

$$U\colon\ (\rho,\phi,z)\rightarrow(\rho,-\phi,-z)\ .$$

If the polymer is invariant with respect to both C_n and U, its line group is $\underline{L}n2=\underline{L}n+(U\,|\,0)\underline{L}n$ and the isogonal point group is $\underline{D}n$. (For n even, the crystallographic convention is to write $\underline{L}n22$.) Since

$$U\,|\,k,m,\lambda\rangle=|\,-k,-m,\lambda\rangle\ , \qquad (9)$$

comparison with (6) shows that U and θ behave the same way on both k and m—they reverse both momenta. Hence, if U is added to C_n and θ (i.e., if the gray line group $\underline{L}^{A}n$ is extended onto $\underline{L}^{A}n2$), there is no change in the degeneracy of the bands. (The same result was indeed obtained along the opposite route[7] when θ was added to C_n and U, i.e., when $\underline{L}n2$ was extended onto $\underline{L}^{A}n2$.)

C. Vertical mirror planes

The mirror-plane reflection σ_v is defined by

$$\sigma_v\colon\ (\rho,\phi,z)\rightarrow(\rho,-\phi,z)\ ;$$

C_n and σ_v together generate the point group $\underline{C}_{nv}$. The corresponding symmorphic line group is $\underline{L}nm=\underline{L}n+(\sigma_v\,|\,0)\underline{L}n$; for n even it is denoted by $\underline{L}nmm$. For a polymer having this symmetry,

$$\sigma_v\,|\,k,m,\lambda\rangle=|\,k,-m,\lambda\rangle\ . \qquad (10)$$

Here, we must distinguish whether m is equivalent to $-m$ or not; the first case happens when $m=\hat{=}$ or $n/2$. Let us consider chiral m first. Since $\epsilon^{\lambda}_{m}(k)=\epsilon^{\lambda}_{-m}(k)$, the two bands with the opposite quasi angular momenta coincide throughout the BZ—there is a twofold band degeneracy. Pictorially, loops such as that in Fig. 2(b) are compressed into double lines.

To illustrate this point, let us consider the model-I polymer of $\underline{L}3$ symmetry (Fig. 4). In a simple tight-binding

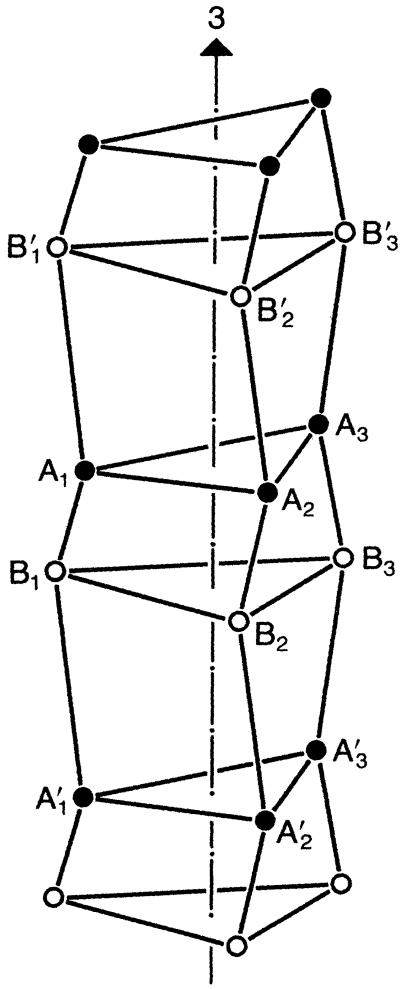

FIG. 4. Model I: a stack of "twisted prisms"; $A_1A_2A_3$ triangles are twisted for an angle θ with respect to $B_1B_2B_3$ triangles. When $\theta\to 0$, the $\underline{L}3$ line-group symmetry of the model increases onto $\underline{L}3m$.

description (one orbital per atom; two-center overlap integrals neglected), for each value of m there are two bands:

$$\epsilon_m^{\pm}(k)=\alpha+2\beta\cos(m\omega)\pm[A+B\cos(m\omega)+C\cos(ka)+D\cos(ka-m\omega)]^{1/2}, \quad (11)$$

where $m=0,\pm1$; $\omega=2\pi/3$; $A=\gamma^2+\delta^2+\eta^2$, $B=2\gamma\delta$, $C=2\gamma\eta$, and $D=2\delta\eta$. The integrals $\alpha,\beta,\ldots,\eta$ are defined as follows:

$$\alpha=\langle A_1|H|A_1\rangle=\langle A_1|H|B_1\rangle ,$$
$$\beta=\langle A_1|H|A_2\rangle=\langle A_1|H|A_3\rangle$$
$$=\langle B_1|G|B_2\rangle=\langle B_1|H|B_3\rangle ,$$
$$\gamma=\langle A_1|H|B_1\rangle,\ \delta=\langle A_1|H|B_2\rangle ,$$
$$\text{and } \eta=\langle A_1|H|B_1'\rangle=\langle B_1|H|A_1'\rangle ;$$

here $|A_1\rangle$ denotes the orbital belonging to the atom A_1, etc. Let us consider only the (lower) ϵ^- bands, dropping the $-$ superscript in what follows; the conclusions about the ϵ^+ bands are completely analogous.

First, it is easily seen from (11) that the ϵ_1 and ϵ_{-1} bands do not coincide, except for $k=0,\pm\pi/a,\ldots$, where they cross; the slopes at these points are

$$\left[\frac{d\epsilon_1}{dk}\right]_0=-\left[\frac{d\epsilon_{-1}}{dk}\right]_0$$
$$=-aD[8(2A+2C-B-D)/3]^{-1/2}, \quad (12a)$$
$$\left[\frac{d\epsilon_1}{dk}\right]_{\pi/a}=-\left[\frac{d\epsilon_{-1}}{dk}\right]_{\pi/a}$$
$$=aD[8(2A-2C-B+D)/3]^{-1/2}. \quad (12b)$$

The extrema are located at general k points,

$$k_{\pm}=(1/a)\arctan[\pm\sqrt{3}D/(2C-D)] \quad \text{for } m=\pm1 . \quad (13)$$

Now let $\delta\to0$ in order to increase the symmetry of the model to $\underline{L}3m$; this corresponds to the untwisting of the upper triangles in Fig. 4 until they are exactly above the lower ones. As seen from (11)–(13), the ϵ_1 and the ϵ_{-1} bands tend towards each other, the extrema move to $k=0,\pm\pi/a,\ldots$, and the slopes at these k points go to zero.

Consider now the ϵ_0 band. It is nondegenerate when $\delta\neq0$, in which case the model has lower, $\underline{L}3$ symmetry; it also remains nondegenerate when $\delta\to0$, and the symmetry increases to $\underline{L}3m$. The extrema are located at $k=0,\pm\pi/a,\ldots$, in either case. The above conclusions are valid generally—for all $m=0$ bands in the case of $\underline{L}nm$ symmetry (n odd) and for all $m=0$ bands and all $m=n/2$ bands in the case of $\underline{L}nmm$ (n even). (Notice that m and $-m$ are equivalent when $m=n/2$, since $m=-m+n$ in that case.)

On the other hand, the nonchiral eigenstates have well-defined parity with respect to the σ_v reflection. We denote the even states by A and the odd ones by B; then,

$$C_n|k,A,0,\lambda\rangle=|k,A,0,\lambda\rangle=\sigma_v|k,A,0,\lambda\rangle , \quad (14a)$$
$$C_n|k,B,0,\lambda\rangle=|k,B,0,\lambda\rangle=-\sigma_v|k,B,0,\lambda\rangle , \quad (14b)$$

and similarly for $m=n/2$, n even. Hence, we have an additional quantum number here, which also characterizes the band as a whole and obeys definite selection rules.[8]

Some physical implications of the results discussed in this section are as follows. If a polymer is symmetric with respect to a rotation C_n (with $n\geq3$) as well as the reflection σ_v, some of the bands are doubly degenerate throughout the BZ. The first-order electron-phonon coupling is thus allowed for some non-totally-symmetric phonons, and one expects a variety of structural instabilities.

The $\underline{L}nm\to\underline{L}n$ symmetry-lowering structural transition causes the selection rules to change. Consequently, some absorption bands disappear from the spectra, since the DOS peaks for chiral m move from $k=0$ and π/a, inwards to certain k_1 and k_2 with $k_1\neq k_2$, in general (be-

cause double $\{m,-m\}$ lines open into single loops), while some new ones appear as the σ_v-parity selection rules for nonchiral states are relaxed. Consequently, uniaxial pressure or electrostatic field could be utilized for assignment of the recorded absorption bands, according to their behavior upon removal of σ_v symmetry.

D. Horizontal mirror planes

The mirror-plane reflection σ_h can be defined by

$$\sigma_h:\ (\rho,\phi,z)\rightarrow(\rho,\phi,-z)\ ;$$

C_n and σ_h generate the point group $\underline{C}_{nh}$. The corresponding symmorphic line group is $\underline{L}n/m=\underline{L}n+(\sigma_h\mid 0)\underline{L}n$. In this case,

$$\sigma_h\mid k,m,\lambda\rangle=\mid -k,m,\lambda\rangle\ , \tag{15}$$

so that σ_h does not affect m, as expected. However, in view of (7),

$$\theta\sigma_h\mid k,m,\lambda\rangle=\mid k,-m,\lambda\rangle\ , \tag{16}$$

so that the combined effect of σ_h and θ is the same as that of σ_v, as given by (10). Hence, for $m\neq 0$ and $n/2$ there is $\{m,-m\}$ degeneracy in this class of polymers also. Here, nonchiral (i.e., $m=0$ or $m=n/2$) states have well-defined parity with respect to σ_h (denoted by the superscript $+$ for even states and by $-$ for odd ones); except for this detail, the discussion is completely analogous to that of Sec. III C.

E. Rotoreflections

If the rotoreflection $S_{2n}\equiv\sigma_h C_{2n}$ is added to $\underline{C}_n$, the point group $\underline{S}_{2n}$ is obtained. The corresponding line group is denoted by $\underline{L}\bar{n}$ for n odd and by $\underline{L}\overline{2n}$ for n even. By itself, S_{2n} cannot affect m since neither of σ_h and C_{2n} does this, so it produces no band degeneracy. It only introduces a parity label which is well defined for every eigenstate,

$$S_{2n}\mid k,m,\pm,\lambda\rangle=\pm\exp(im\alpha/2)\mid -k,m,\pm,\lambda\rangle\ . \tag{17}$$

However, as in Sec. III D, here θS_{2n} reverts m into $-m$ while not affecting k, and thus produces twofold band degeneracy for every $m\neq 0$. Notice that the $m=n/2$ case is included here, since θ transforms even states into odd ones; the rest is analogous to Sec. III C.

F. Point groups $\underline{D}_{nd}$

In this section we have studied the $\underline{C}_n$ point group first, and then its minimal extensions, i.e., groups of the form $\underline{C}_n+R\underline{C}_n$, where $R=U$, σ_v, σ_h, or S_{2n}. The point group $\underline{D}_{nd}$ is an extension of an extension: $\underline{D}_{nd}=\underline{C}_{nv}+U_d\underline{C}_n$ or equivalently $\underline{D}_{nd}=\underline{S}_{2n}+\sigma_v\underline{S}_{2n}$. The corresponding symmorphic line groups are $\underline{L}\bar{n}m$ (n odd) and $\underline{L}(\overline{2n})2m$ (n even). Since they contain both C_n and σ_v, each band having quasi angular momentum m coincides with one having $-m$ provided that $m\neq 0$ and $n/2$ (cf. III C). It is easy to verify that θU_d maps states even with respect to σ_v (A states) into even states, if $m=0$, and into odd ones (B states) for $m=n/2$; hence, the $m=0$ bands are nondegenerate, while the $m=n/2$ bands are twofold degenerate. These conclusions are obvious also in view of Sec. III E, since $\underline{D}_{nd}$ contains $\underline{S}_{2n}$ as a subgroup.

G. Point groups $\underline{D}_{nh}$

The last remaining family of finite axial point groups is $\underline{D}_{nh}=\underline{C}_{nv}+\sigma_h\underline{C}_{nv}$, $n=1,2,\ldots$; the corresponding symmorphic line groups are $\underline{L}(\overline{2n})2m$ (n odd) and $\underline{L}n/mmm$ (n even). Since σ_h does not change the parity (with respect to σ_v) of $m=0$ and $n/2$ eigenstates, the discussion is completely analogous to that of Sec. III C.

H. Straight atomic chains

In a special case, when all the atoms that form the chain lie on the same axis, the polymer is invariant with respect to any rotation around its axis and any mirror plane containing that axis. The point group is a continuous one, $\underline{C}_{\infty v}=\underline{C}_\infty+\sigma_v\underline{C}_\infty$, and the line group is $\underline{L}\infty m$. Here, $m=m_z=0,\pm1,\pm2,\ldots$; the bands with $m=0$ are nondegenerate and all the others are twofold degenerate (cf. Sec. III C).

A horizontal mirror plane is another possible symmetry element of a straight chain of atoms. In that case, one has $\underline{D}_{\infty h}$ and $\underline{L}\infty/mm$; the above conclusions remain valid, in analogy with Sec. III G.

As a simple example, consider a chain of equidistant carbon atoms in the tight-binding approximation and with the same simplifying assumptions as in Sec. III C. Two nondegenerate ($m=0$) bands arise from $2s$ and $2p_z$ atomic orbitals while $2p_x$ and $2p_y$ generate one twofold-degenerate $\{m=1,m=-1\}$ band.

IV. HELICES: SCREW AXES

Stereoregular polymers, either synthetic or natural, are most frequently found in the form of helices. They are built out of monomers which may consist of one atom (as in selenium, tellurium, or polymeric sulfur) or of many atoms. The number of monomers per one translation period can also vary considerably. In general,[6] such a helix is invariant with respect to some $(C_n\mid p/n)$ with $p=0,1,\ldots,n-1$, and the corresponding line group is denoted by $\underline{L}n_p$; every periodic helical polymer can be characterized in this way.[6] The eigenfunctions are of the form

$$\psi_{km}(\vec{r})=\exp(ikz)\exp(im\phi)u(\rho,\phi,z)\ , \tag{18a}$$

with

$$u(\rho,\phi,z)\equiv u(\rho,\phi-2\pi/n,z-pa/n)\ , \tag{18b}$$

where $-\pi/a<k\leq\pi/a$ and m is given by (2). Since (18a) coincides with (4a), many of the results of Sec. III retain their validity here. The eigenstates are labeled by the quantum numbers k and m, which behave under the action of symmetry operators as expected from their physical interpretation: $[C_n\mid p/n]$ changes neither k nor m, σ_v reverts m into $-m$, σ_h reverts k into $-k$, while U and θ revert both k and m. However, (18b) does not coincide with (4b); $\underline{L}n_p$ is a nonsymmorphic line group and it does

not contain $(C_n \mid 0)$ as an element. Rather, the C_n rotation is in $\underline{L}n_p$ coupled to a (fractional) translation $(p/n)a\vec{e}_z$, so that k and m are coupled also, as manifested by the following umklapp theorem:

$$|k,m,\lambda\rangle = |k+2\pi/a, m-p, \lambda'\rangle \ , \tag{19}$$

with $\lambda \neq \lambda'$, in general. Combining (19) with (6), we conclude that

$$\epsilon_\lambda(0,m) = \epsilon_\lambda(0,-m) \ , \tag{20a}$$

and

$$\epsilon_\lambda(\pi/a,m) = \epsilon_\lambda(-\pi/a,-m) = \epsilon_{\lambda'}(\pi/a,-m-p) \ . \tag{20b}$$

Hence, at $k=0$ the bands with $m=0$ and (for even n) with $m=n/2$ remain nondegenerate, while the others cross pairwise; the intersecting bands have opposite quasi angular momenta. These results are identical to those of Sec. III A as expected, because the fractional translations become negligibly small compared to the wavelength when $k \to 0$. However, the situation is very different at $k=\pi/a$; a band with quasi angular momentum m crosses another with $m'=-m-p$ (instead of $-m$). The bands that remain nondegenerate are those for which $m=m'$, i.e., those with $m=-p/2$ when p is even, and those with $m=(n-p)/2$ when $n-p$ is even. In the case of $\underline{L}3_1$, for example, the $m=0$ bands are nondegenerate and each $m=1$ band intersects an $m=-1$ band at $k=0$. At $k=\pi/a$, the $m=1$ bands are nondegenerate; the $m=0$ bands intersect those with $m=-1$. For $\underline{L}4_2$ symmetry, bands with $m=1$ or -1 are nondegenerate, and $m=0$ bands cross $m=2$ bands at $k=\pi/a$, etc.

Similar conclusions apply for the selection rules. For direct optical absorption, one has $\Delta k=0$, and hence $\Delta \doteq \mu$ (where Δk, Δm, and μ have the same meaning as in Sec. III A) and there is no difference between $\underline{L}n$ and $\underline{L}n_p$. However, in umklapp processes, k increases by a reciprocal-lattice vector, and m—being coupled to k—changes also, according to (19) instead of (6); hence, in this case the selection rules for $\underline{L}n_p$ do not coincide with those for $\underline{L}n$.

The above results apply for every screw-axis symmetry, but to obtain more physical insight we must distinguish whether n and p are relatively prime integers or not and discuss each case separately.

A. Simple helices: cyclic screw axes

When n and p are relatively prime the $\underline{L}n_p$ line group is cyclic, i.e., it consists of all (positive and negative) powers of certain $(C_n^s \mid 1/n)$, where s is determined by n and p. Consequently, the chain contains n monomers per angle $2s\pi$, i.e., per s turns of the helix. (It is usual in polymer literature to denote such a helix by n/s; notice that it does not necessarily correspond to n_s. For example, 7/2 correponds to 7_4.)

The 1D translation group is also a cyclic one, and on the basis of this isomorphism one concludes[14] that if H commutes with $\underline{L}n_p$, its eigenfunctions are of the form $\exp(iqz)u(\vec{r})$ with $q \in (-n\pi/a, n\pi/a]$. To switch back to the usual k space description, one just folds the q space band structure n times. However, each $\epsilon_\lambda(q)$ is a smooth function of q throughout the large zone [referred to as JZ in solid-state physics), so that folding automatically produces some band coherence at the center and/or at the edges of the BZ.

As an illustration, consider a helix with three atoms per one turn, model II [Fig. 5(a)]. If each atom contributes one orbital, the tight-binding energy bands are given by

$$\epsilon_m(k) = \alpha + 2\beta\cos(ka/3 + 2m\pi/3) \ ,$$

where $m=0,\pm 1$. These three bands [Fig. 5(c)] connect in the way described earlier in this section ($m=1$ with $m=-1$ at $k=0$; $m=0$ with $m=-1$ at $k=\pi/a$) and indeed unfold into a single smooth line in the JZ [Fig. 5(b)]. Yet another equivalent graphical representation is given in Fig. 5(d): three curves each with period $6\pi/a$ (equal to the width of the JZ), thread in such a way that the figure as a whole has period $2\pi/a$ (the width of the BZ). The DOS has two peaks [Fig. 5(e)] which correspond to the states $|0,0\rangle$ and $|\pi/a,1\rangle$.

In most linear combination of atomic orbitals—type (LCAO) calculations, one deals with more than one orbital per atom, so that band structures are more complex, but above conclusions about connectivity remain valid. The role of symmetry labels becomes, in fact, more important, since they determine which of the possible band crossings are allowed. To illustrate this point, let us consider the same model II, but with two orbitals per atom, for example, p_r and p_t. The relevant matrix elements are $\alpha = \langle p_r \mid H \mid p_r\rangle = \langle p_t \mid H \mid p_t\rangle$, $\beta_r = \langle p_r \mid G \mid p_r'\rangle$, $\beta_t = \langle p_t \mid H \mid p_t'\rangle$, and $\gamma = \langle p_r \mid H \mid p_t'\rangle = \langle p_t \mid H \mid p_r'\rangle$, where the prime denotes orbitals on a neighboring atom. The bands are given by

$$\epsilon_m^{\pm}(k) = \alpha + (A \pm B)\cos(ka/3 + 2m\pi/3) \ ,$$

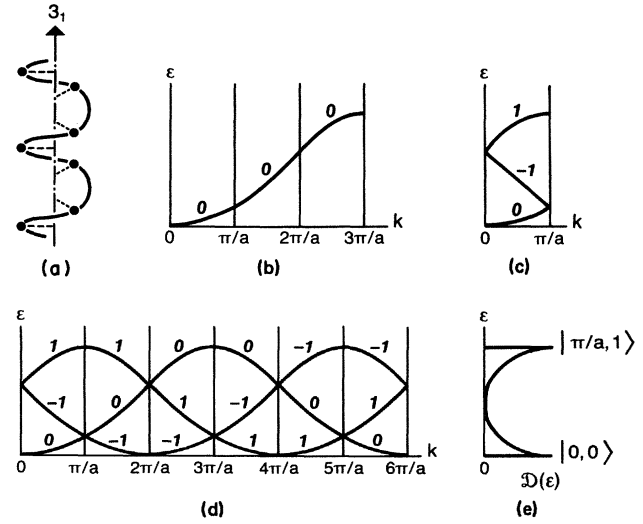

FIG. 5. (a) Model II: a simple monatomic 3_1 helix. (b) Its (tight-binding) bands are smooth in the JZ; (c) they fold twice to form S shapes in the BZ and (d) make triple threads in the extended-zone model. (e) The DOS peaks correspond to $k=0$ for $m=0$ bands, and to $k=\pi/a$ for $m=1$ bands.

where $A=\beta_r+\beta_t$ and $B=[4\gamma^2+(\beta_r-\beta_t)^2]^{1/2}$. In the band structure sketched in Fig. 6, we observe three band crossings, two of which are allowed (because the intersecting bands have different quasi angular momenta), while the middle one should be avoided as indicated in Fig. 6. Notice, however, that before a crossing is ruled out, one should check whether there are any additional symmetry labels that could differ for the two bands considered. Hence, it is important to analyze the effects of other possible symmetry elements; we do this in Sec. IV C.

The above considerations are easily generalizable to arbitrary cyclic $\underline{L}n_p$. Bands always group in sets of n threading lines, each one having period $2n\pi/a$. The DOS peaks correspond to $|0,0,\lambda\rangle$ and $|0,n/2,\lambda\rangle$ if n is even, to $|0,0,\lambda\rangle$ and $|\pi/a,-p/2,\lambda\rangle$ if p is even and n is odd, and to $|0,0,\lambda\rangle$ and $|\pi/a,(n-p)/2,\lambda\rangle$ if both n and p are odd.

Some related results in solid-state physics could be mentioned here. Within a nearly free-electron approximation, the width of the gap between two bands at the BZ edge is related to the Fourier-expansion coefficients of the period potential. Lax[5] found that some space-group symmetry elements necessitate certain coefficients, and hence the band gaps, to vanish. The application of his reasoning to the $\underline{L}n_p$ line-group symmetry leads to the same conclusions as given above. Another approach is to view the zero-velocity states as standing waves, and to look for $\lambda=2\pi/k$, which satisfies the Bragg diffraction condition.[15] If a simple $\underline{L}n_p$ helix is projected onto the z axis, identical atoms are found at a/n vertical distance, and one indeed expects $\delta\epsilon/\delta k=0$ for $k=2\pi/\lambda=n\pi/a$.

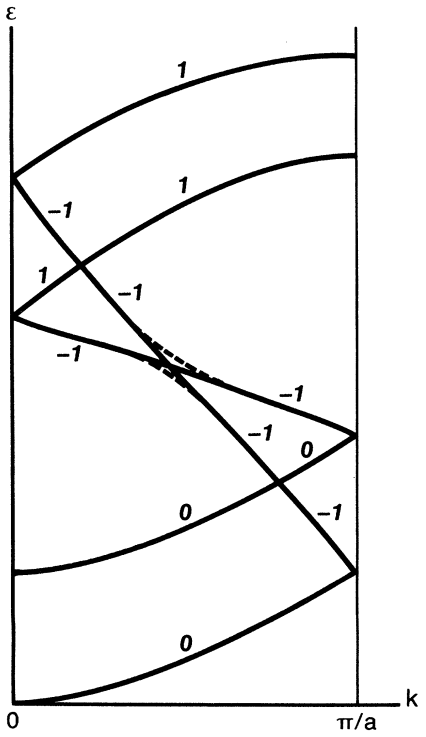

FIG. 6. Bands for model II [see Fig. 5(a)], but with two orbitals per atom: two S shapes are formed, with one avoided and two allowed crossings.

B. Multiple helices: noncyclic screw axes

Let us now consider the remaining $\underline{L}n_p$ line groups for which n and p are not relatively prime. In other words, let $n=n'r$ and $p=p'r$ with n' and p' relatively prime, but now let $r\geq 2$. In this case (i) the smallest fractional translation to appear in an element of $\underline{L}n_p$ is $(1/n')a\vec{e}_z$, and (ii) $\underline{L}n_p$ contains some proper rotations, viz. $(C_r\,|\,0),\ldots,(C_r^{r-1}\,|\,0)$. Let us clarify this point by a few examples. The line group

$$\underline{L}4_2=\{\ldots,(E\,|\,0),(C_4\,|\,1/2),(C_2\,|\,0),\ (C_4^3\,|\,1/2),(E\,|\,1),(C_4\,|\,3/2),\ldots\}$$

is not a cyclic one, since $(C_4\,|\,1/2)$ generates only its proper subset

$$\underline{L}'4_1=\{\ldots,(C_4\,|\,1/2),(C_2\,|\,1),(C_4^3\,|\,3/2),\ (E\,|\,2),(C_4\,|\,5/2),\ldots\}\ .$$

This set becomes identical to the cyclic line group $\underline{L}4_1$ if the translational period is doubled; from an atom (which is not on the z axis), $\underline{L}'4_1$ generates a simple helix with four atoms per period, which equals $2a$. Now, $\underline{L}4_2=\underline{L}'4_1+(C_2\,|\,0)\underline{L}'4_1$, since $(C_2\,|\,0)$ rotates every atom by π around the z axis, it generates the second simple helix. In this sense noncyclic $\underline{L}n_p$ line groups describe multiple helices. Thus $\underline{L}6_2=\underline{L}'6_1+(C_2\,|\,0)\underline{L}'6_1$ again describes a double helix, while $\underline{L}6_3=\underline{L}'6_1+(C_3\,|\,0)\underline{L}'6_1+(C_3^2\,|\,0)\underline{L}'6_1$ and $L9_3=\underline{L}'9_1+(C_3\,|\,0)\underline{L}'9_1+(C_3^2\,|\,0)\underline{L}'9_1$ correspond to triple helices (each one having period $3a$), etc.

In view of (i) and (ii), we expect the JZ width to be $n'2\pi/a$, here, and also, some effects of the $\underline{C}_r$ rotational symmetry to be felt. This is illustrated in Fig. 7, where the band-connectivity schemes are given for $\underline{L}4_2$ and $\underline{L}6_3$ line groups, respectively. The minimal fractional translation is $(1/2)a\vec{e}_z$ and the width of the JZ is $4\pi/a$, in either case. The $\underline{L}4_2$ example illustrates that a screw axis does not always necessitate that all the bands cross pairwise at $k=\pi/a$, contrary to what can be found in the literature; indeed, a semicross appears in certain cases [viz. for $\underline{L}(2q)_q$ line groups with $q=1,2,\ldots$, for the bands with $m\neq 0$ and $m\neq q$]. The $\underline{L}6_3$ example illustrates that for $r\geq 3$ a loop in the JZ appears as a consequence of the $\underline{C}_r$ rotation symmetry, which then folds onto a butterfly diagram in the BZ. This butterfly is essential, since the bands that intersect have different quasi angular momenta and the crossing is allowed. It thus produces two DOS peaks, in contrast to the inessential butterfly in Fig. 4(b), which gives rise to four peaks. A similar loop is found in the case of $\underline{L}9_3$ helix also, but the JZ width is $6\pi/a$ and the loop folds twice, so that a more complex diagram results.

C. Additional symmetry elements: rotation axes and mirror planes

Let us consider dihedral axes first. As seen from (6) and (9), U and θ act in the same way on k and m. In Secs. IV A and II B we have analyzed the combined effects of n_p screw-axis symmetry and time-reversal invariance, i.e.,

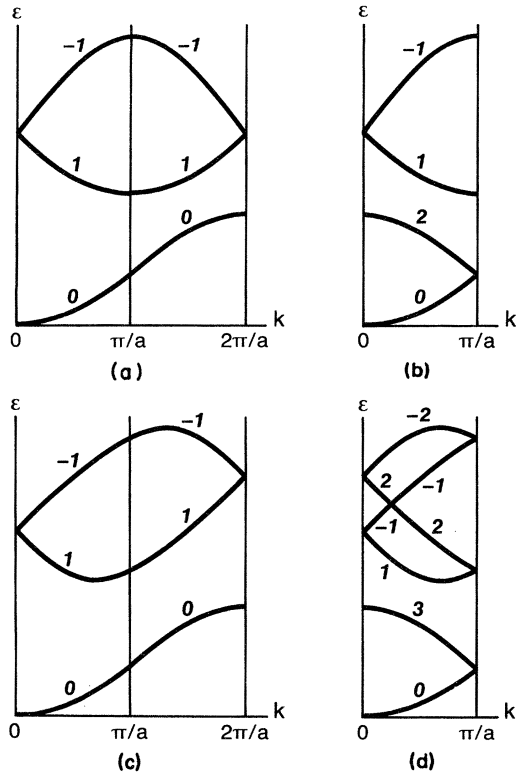

FIG. 7. (a) JZ band shapes and (b) BZ band shapes for an $\underline{L}4_2$ helix; (c) and (d) the same for an $\underline{L}6_3$ helix.

of the group $\underline{L}^A n_p$. We can now extend it onto $\underline{L}^A n_p 2 = \underline{L}^A n_p + (U \mid 0)\underline{L}^A n_p$ (this extension is denoted by $\underline{L}^A n_p 22$ for n even) without any change in degeneracy. Precisely because of this fact, it was possible to restrict ourselves to the $\underline{L}^A 3_1$ group in the study of the band structure of the monatomic chain example in Sec. IV A, although the symmetry group of the model is $\underline{L}^A 3_1 2$.

Turning now to possible reflection-plane symmetries, we first[6] notice that they are compatible with n_p screw-axis symmetry only if n is even and $p = n/2$. In that case, a vertical mirror plane can be present, or a horizontal one, or both of them; the corresponding line groups are $\underline{L}(2q)_q mc$, $\underline{L}(2q)_q/m$, and $\underline{L}(2q)_q/mcm$, respectively. In either case, (i) the minimal fractional translation to appear in the group is $(1/2)a\vec{e}_z$ and the width of the JZ is $4\pi/a$; (ii) the bands with chiral quasi angular momentum (i.e., with $m \neq 0$ and $m \neq q$) are all twofold degenerate throughout the BZ—for every band labeled by m there is a coincident one with label $-m$; (iii) each $\{m,-m\}$ double line has a zero slope at $k=0$; (iv) at $k=\pi/a$, each $\{m,-m\}$ double band intersects (at nonzero slope) an $\{\bar{m},-\bar{m}\}$ band, with $\bar{m} = q-m$, unless $m = q/2$; (v) for even q, each $\{q/2,-q/2\}$ double band has a zero slope at $k=\pi/a$; (vi) nonchiral (i.e., $m=0$ and q) bands are all nondegenerate at $k=0$ and inside the BZ; and (vii) nonchiral bands intersect pairwise at $k=\pi/a$—an A_0 (B_0) band crosses an A_q (B_q) band. All these results can be obtained by easy manipulations with k and m, as follows from (6), (10), (16), and (19). The main consequence of replacing a rotation axis by a screw axis is that the umklapp-change rule for m is given by (19) instead of (7). This is felt essentially at the BZ boundaries, as seen from (i), (iv), and (vii) above; otherwise, the results coincide with those of Secs. III C, III D, and III G. Hence, the comments given there can be rephrased here also—e.g., a double semiloop will open into a butterfly upon removal of mirror-plane symmetry, and the selection rules will change subsequently. Notice also that in view of (iv) the high, fourfold band degeneracy (in the orbital space; with spin included the degeneracy if eightfold) is encountered here.

V. ALTERNATING STACKS: GLIDE PLANES

The remaining symmetry element to be considered is the reflection with respect to a plane containing the polymer axis followed by the fractional translation $(1/2)a\vec{e}_z$, i.e., the glide plane $(\sigma_v \mid 1/2)$. Certain stereoregular polymers do have this symmetry; it may also appear when some identical objects (e.g., molecules) are stacked so that they are oriented to the left and to the right in alternation.

The simplest line group containing a glide plane is $\underline{L}1c$; it is in fact the cyclic group generated by $(\sigma_v \mid 1/2)$. In this case the eigenstates are characterized by two quantum numbers, the quasimomentum k, and the parity with respect to $[\sigma_v \mid 1/2]$, defined by

$$[\sigma_v \mid 1/2] \mid k,A,\lambda\rangle = \kappa \mid k,A,\lambda\rangle \ , \tag{21a}$$

$$[\sigma_v \mid 1/2] \mid k,B,\lambda\rangle = -\kappa \mid k,B,\lambda\rangle \ , \tag{21b}$$

where $\kappa = \exp(-ika/2)$ and $-\pi/a < k \leq \pi/a$; λ enumerates bands of the same parity, in order of ascending energy at $k=0$. The information that we need about these eigenstates is how they transform upon the time reversal:

$$\theta \mid k,A,\lambda\rangle = \mid -k,A,\lambda\rangle \ , \tag{22a}$$

$$\theta \mid kB\lambda\rangle = \mid -k,B,\lambda\rangle \ , \tag{22b}$$

and the umklapp theorem:

$$\mid k,A,\lambda\rangle = \mid k+K,B,\lambda\rangle \ , \tag{23a}$$

$$\mid k,B,\lambda\rangle = \mid k+K,A,\lambda\rangle \ , \tag{23b}$$

where $K = \pm 2\pi/a$.

Together, (22) and (23) imply that all the bands group into pairs forming semiloops in the right half of the BZ. All the bands are nondegenerate and have a zero slope at $k=0$, and they remain nondegenerate as k increases up to $k=\pi/a$, where they cross pairwise (an A band intersects a B band at nonzero slope). The period of each curve is $4\pi/a$, and the JZ is twice as large as the BZ. All these results are in fact expected from the analogy to those for the $\underline{L}2_1$ line group, which is isomorphous to $\underline{L}1c$. Indeed, in some more complex line groups, other symmetry elements appear together with glide planes; we consider them in what follows.

A. Glide planes combined with a rotation axis

The $(\sigma_v \mid 1/2)$ glide-plane symmetry and $(C_n \mid 0)$ rotations are compatible for arbitrary n; the line groups generated by these two elements are denoted by $\underline{L}nc$ for n odd

and by $\underline{L}ncc$ for n even. In either case, there are three symmetry-generated quantum numbers characterizing the eigenstates—the quasimomentum k, the quasi angular momentum m, and, only for nonchiral states, the parity with respect to $[\sigma_v \mid 1/2]$. Band structures contain double semiloops formed by pairs of $\{m,-m\}$ double bands, and single semiloops formed by nonchiral bands—A_0 (A_q) bands intersect with B_0 (B_q) bands, respectively, at $k=\pi/a$. These conclusions about the band shapes result from the following facts. (i) Time inversion reverts both k and m here, as in (6), while it does not affect the parity with respect to $[\sigma_v \mid 1/2]$, as in (22a) and (22b). (ii) $[\sigma_v \mid 1/2]$ does not change k, but it reverts m, since $[\sigma_v \mid 1/2] \mid k,m,\lambda\rangle = \exp(-ika/2) \mid k,-m,\lambda\rangle$. (iii) In umklapp processes the quasi angular momentum m is not changed, as in (7), while the parity with respect to $[\sigma_v \mid 1/2]$ is reversed, as in (23a) and (23b), so that $\theta \mid \pi/a,A,q,\lambda\rangle = \mid -\pi/a,A,q,\lambda\rangle = \mid \pi/a,B,q,\lambda\rangle$, etc. (iv) $\mid \pi/a,m,\lambda\rangle$, $\theta \mid \pi/a,m,\lambda\rangle$, $[\sigma_v \mid 1/2] \mid \pi/a,m,\lambda\rangle$, and $\theta[\sigma_v \mid 1/2] \mid \pi/a,m,\lambda\rangle$ are linearly independent. Notice that (iv) implies fourfold (orbital) band degeneracy although only two (opposite) values of quasi angular momentum are involved, in contrast to the situation in Sec. IV C, where four different values of m have been included. Observe also that the $(1/2)a\vec{e}_z$ fractional translation makes the JZ width equal to $4\pi/a$ here, as in the case of $\underline{L}1c$.

B. Other symmetry elements

There are four more families of line groups that contain glide planes. Two of these, $\underline{L}(2q)mc$ and $\underline{L}(2q)_q/mcm$, have been considered already, in Sec. IV C; glide planes appear in them as a result of combining the $(2q)_q$ screw axis with the $(\sigma_v \mid 0)$ mirror plane. Next, the results for the line groups $\underline{L}(\overline{2n})2c(n$ odd) and $\underline{L}n/mcc$ (n even) coincide with those for $\underline{L}nc$ and $\underline{L}ncc$, respectively. Namely, $[\sigma_h \mid 0]$ preserves the parity with respect to $[\sigma_v \mid 1/2]$, and thus it introduces no additional degeneracies; compare also Sec. III G. Finally, there are $\underline{L}\bar{n}c$ (n odd) and $\underline{L}(\overline{2n})2c$ (n even) line groups, isogonal to $\underline{D}_{nd}$. In contrast to the preceding case, $[U_d \mid 0]$ does revert the parity with respect to $[\sigma_v \mid 1/2]$ if the state has the quasi angular momentum $m=q$, i.e., $\theta[U_d \mid 0] \mid k,A,q,\lambda\rangle = \mid k,B,q,\lambda\rangle$, as in Sec. III F. Consequently, each A_q band becomes degenerate throughout the BZ to a B_q band, and zero sloped at $k=0, \pm\pi/a,\ldots$. Shapes of the other bands are not affected. This covers all the line groups.

VI. APPLICATION: VIBRONIC COUPLING IN POLYMERS

Vibronic coupling becomes important in the case of electronic degeneracy in molecules, where it can cause point-group symmetry breaking,[16] as well as in linear atomic chains with partially filled conduction bands, where it causes translational symmetry breaking.[17] In Secs. III—V we have seen many examples of electronic degeneracy in polymers; in that case, vibronic coupling can cause line-group symmetry breaking. We let $\mid \psi_i\rangle$, $i=1,\ldots,d$ denote the degenerate electronic states and Q denote a small displacement of the nuclei from the initial configuration; then, in general,

$$\left\langle \psi_i \left| \left[\frac{\partial V}{\partial Q} \right]_0 \right| \psi_j \right\rangle \neq 0 \quad (i,j=1,\ldots,d) \tag{24}$$

for some non-totally-symmetric Q. If $\mid \psi_i\rangle$, $i=1,\ldots,d$ belong to a representation D of the line group $\underline{L}$ of the polymer under study, one can determine the active modes Q by decomposing the Kronecker square $[D^2]$, as in Ref. 16. However, despite a complete analogy with the mentioned classic results of Jahn and Teller[16] and Peierls,[17] more comprehensive work still must be done—the line groups contain rotations and/or reflections as well as translations, and thus in polymers the situation is somewhat more complex. Indeed, it turns out that the vibronically active phonons in Q1D solids can be transversal as well as longitudinal, distortive, or displacive (both ferro- and antiferro-), nondegenerate or degenerate, etc.; furthermore, several modes are interplaying in most cases. The active modes are essentially determined by the line group $\underline{L}$, by the band shape(s) involved, and by the quantum numbers (k and m, the parities with respect to σ_v, σ_h, etc.) of the degenerate electronic states at the Fermi level ϵ_F. These concepts have been described in detail in Secs. III—V; let us now illustrate how useful they are in some applications.

The total electronic energy of a polymer is degenerate when a band shape is partially filled, so let us analyze several typical cases—a single line, a semiloop, and a double line, assuming for simplicity that they are exactly one-half filled. To be less abstract, two simple model polymers are considered, each with four atoms per unit cell. Model III is an equidistant array of square planar molecules in the eclipsed positions [Fig. 8(a)], and model IV is a staggered array of diatomic molecules [Fig. 9(a)].

Model III has $\underline{L}4/mmm$ line-group symmetry. Since $\underline{L}4/mmm = \underline{L}4mm + (\sigma_h \mid 0)\underline{L}4mm$, and since $(\sigma_h \mid 0)$ introduces only $\{k,-k\}$ star degeneracy, one can label the bands by quantum numbers of $\underline{L}4mm$ (see Secs. III C and III G). For simplicity, let each atom contribute only one atomic orbital of the $l=0$ (i.e., s, p_z, d_{z^2}, etc.) type; then, the tight-binding energy bands of this polymer are given by

$$\epsilon({}_kA_0) = \alpha + 2\beta + 2\gamma\cos(ka)\,, \tag{25}$$

$$\epsilon({}_kA_2) = \alpha - 2\beta + 2\gamma\cos(ka)\,, \tag{26}$$

$$\epsilon({}_kE_{1,-1}) = \alpha + 2\gamma\cos(ka)\,, \tag{27}$$

where $\alpha = \langle 1 \mid H \mid 1\rangle$, $\beta = \langle 1 \mid H \mid 2\rangle$, and $\gamma = \langle 1 \mid H \mid 5\rangle$, and where $\mid 1\rangle$ denotes the atomic orbital centered at atom 1 [see Fig. 8(a)], etc. Of these three bands, the first two are nondegenerate (single lines), while the last one is twofold degenerate throughout the BZ (a double line). To facilitate discussion, let us assume that there is no overlap among these three bands; that is the case when $\mid \gamma \mid < \mid \beta \mid /2$.

Model IV has $\underline{L}4_2/mcm = \underline{L}4_2mc + (\sigma_h \mid 0)\underline{L}4_2mc$ line-group symmetry. The quantum numbers of $\underline{L}4_2mc$ are the same as for $\underline{L}4mm$; see Sec. IV C. With the same asumptions as in the preceding case, the electronic energy bands are given by

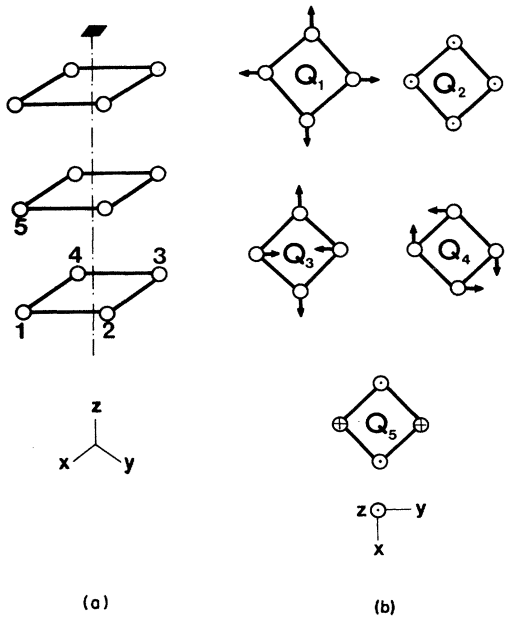

FIG. 8. (a) Model III: a stack of square planar molecules. (b) Some of its vibration modes relevant for the present discussion.

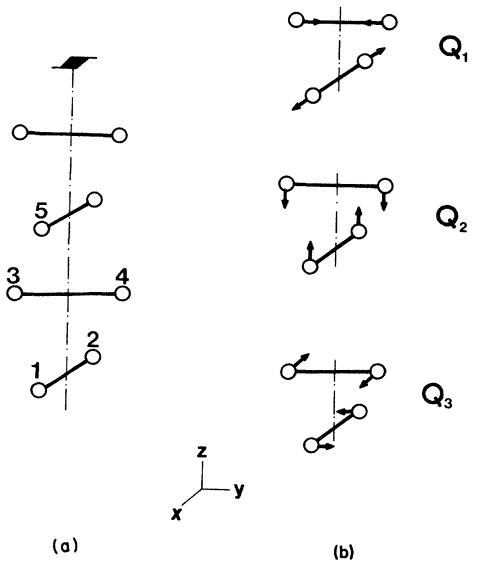

FIG. 9. (a) Model IV: a staggered array of diatomic molecules; (b) its relevant vibration modes.

$$\epsilon({}_kA_0)=\alpha+\beta+2\delta\cos(ka)+4\gamma\cos(ka/2)\,, \tag{28}$$

$$\epsilon({}_kA_2)=\alpha+\beta+2\delta\cos(ka)-4\gamma\cos(ka/2)\,, \tag{29}$$

$$\epsilon({}_kE_{1,-1})=\alpha-\beta+2\delta\cos(ka)\,, \tag{30}$$

where $\alpha=\langle 1\,|\,H\,|\,1\rangle$, $\beta=\langle 1\,|\,H\,|\,2\rangle$, $\gamma=\langle 1\,|\,H\,|\,3\rangle$, and $\delta=\langle 1\,|\,H\,|\,5\rangle$; for the atomic labels see Fig. 9(a). Notice that δ is an interaction between the next-nearest neighbors, and hence smaller than β or γ in general; if $\delta\to 0$, the degenerate E band becomes completely flat. If we assume again that $|\gamma|<|\beta|/2$, the E band does not overlap with the other two bands, A_0 and A_2; the latter two, however, necessarily cross each other at $k=\pi/a$. Hence, we have here an example of a semiloop [as in Fig. 1(b)] and a separate, narrow double line.

A. One-half-filled single line

Let us first consider the case when the lowest A_0 band of model III is one-half-filled; then, there is a twofold, $\{k_F,-k_F\}$-star degeneracy at ϵ_F, in close analogy to the Peierls model. The involved degenerate electronic states are $|\,{}_{\pi/2}A_0\rangle$ and $|\,{}_{-\pi/2}A_0\rangle$, and hence a nontrivial (i.e., symmetry-reducing) active mode must have quasimomentum $q=\pi/a$, quasi angular momentum $\mu=0$, and it must be even (A mode) with respect to σ_v; there are no restrictions concerning its parity with respect to σ_h. Indeed, the active modes are the ${}_\pi Q_1$ mode of ${}_\pi A_0^+$ symmetry, and the ${}_\pi Q_2$ mode of ${}_\pi A_0^-$ symmetry. Their geometries can be inferred from Fig. 8(b), where the Q_1 and Q_2 modes of a single square molecule are illustrated; the index π indicates that $q=\mp\pi/a$, i.e., that neighboring squares move out-of-phase.

One can now proceed to determine the reduced-symmetry group $\underline{L}_Q$ of the polymer distorted by either ${}_\pi Q_1$ or ${}_\pi Q_2$, and then to infer from $\underline{L}_Q$ whether and how the band shapes change upon distortion. Since neither of these two modes reduces the point-group symmetry of individual molecules, but only reduces the translational symmetry of their arrangement, the new line group is $\underline{L}'4/mmm$, where the prime indicates that the period is doubled, $a'=2a$. The width of the new BZ is thus π/a, one-half the original width; each band is folded once and simultaneously a gap opens in it at $k=\pi/2a$, so that altogether four single and two double lines are formed. In particular, a gap opens at k_F and the star degeneracy of this level is lifted, since each state at $k=-\pi/2a$ is now equivalent to a state at $k=\pi/2a$.

To conclude, this chain is unstable with respect to a mode belonging to the longitudinal-acoustic (LA) vibration branch (the ${}_\pi Q_2$ mode), just as the Peierls model; however, in the present case there is an additional instability against a mode from a transverse-optical (TO) branch, the ${}_\pi Q_1$ mode. Such an instability was investigated recently[18] by Feinberg and Ranninger, whose model polymer has a lateral degree of freedom; in the present model both instabilities are present and they compete in general.

Another example of a single line is the highest A_2 band of model III. If that band is the one-half-filled one, all the above conclusions remain valid. Even the active modes are the same; this follows from the quantum numbers of the degenerate electronic states.

B. One-half-filled semiloop

For the next example, let us analyze the case when the semiloop formed by the A_0 band and the A_2 band of model III, as given by (28) and (29), is one-half filled. Then the Fermi level is at $k_F=\pi/a$ and it is twofold-band degenerate because of the band crossing. The degenerate states, $|\,{}_\pi A_0\rangle$ and $|\,{}_\pi A_2\rangle$, can be mixed by a phonon with $q=0$ and $\mu=2$, and which is even with respect to σ_v; the σ_h parity is not restricted. The active modes are ${}_0Q_1$ and

${}_0Q_2$ [Fig. 9(b)], of ${}_0A_2^+$ and ${}_0A_2^-$ symmetry, respectively. Each of these two modes distorts the polymer into a configuration of $\underline{L}2/mmm$ symmetry; the band shapes change into four single lines (the E band splits into two nondegenerate bands, and a gap opens at $k_F=\pi/a$, between the A_0 band and the A_2 band), so that the band degeneracy is completely lifted. The active modes, the antiferrodisplacive ${}_0Q_2$ mode, and the antiferrodistortive ${}_0Q_1$ mode, again resemble the Peierls and the Feinberg-Ranninger mode, respectively [see Fig. 9(b)]. However, the difference is that in the present case both modes are optical (${}_0Q_2$ is an LO mode and ${}_0Q_1$ is a TO mode) and fundamental (i.e., with $q=0$), so that the translation repeat length a remains unaltered. In fact, the point-group symmetry of individual molecules is also preserved, and here one has a very specific type of symmetry breaking, in which a nonsymmorphic symmetry element, $(C_4 \mid 1/2)$, is lost.

C. One-half-filled double line

Finally, let the twofold-degenerate $E_{1,-1}$ band of model III, as given by (27), be one-half filled, so that the degenerate states at ϵ_F are $|\psi_1\rangle=|\pi/2;1\rangle$, $|\psi_2\rangle=\sigma_v|\psi_1\rangle=|\pi/2;-1\rangle$, $|\psi_3\rangle=\sigma_h|\psi_1\rangle=|-\pi/2;1\rangle$, and $|\psi_4\rangle=\sigma_h|\psi_2\rangle=|-\pi/2;-1\rangle$. Let us now determine the active vibrational modes which illustrates well the simplicity of the present method.[19]

To facilitate the discussion, let us utilize the coordinate representation. In view of (6), (10), and (15), $\psi_1^*=\psi_4$ and $\psi_2^*=\psi_3$, so that out of the 16 products $\psi_i^*\psi_j$ $(i,j=1,\ldots,4)$, only 10 are linearly independent. It is convenient to retain the 10 products $\psi_i\psi_j$, $i\le j$, whose symmetry-generated quantum numbers are easily determined from those of ψ_i and ψ_j. For example, the function $\psi_1\psi_2$ has the total quasimomentum $q=\pi/a$, the total quasi angular momentum $\mu=0$, and it is even with respect to σ_v; however, it is not invariant with respect to σ_h, since $\sigma_h(\psi_1\psi_2)=(\sigma_h\psi_1)(\sigma_h\psi_2)=\psi_3\psi_4$. But one can replace $\psi_1\psi_2$ and $\psi_3\psi_4$ by the functions $f=(\psi_1\psi_2+\psi_3\psi_4)/2$ and $g=(\psi_1\psi_2-\psi_3\psi_4)/2$, which are even and odd with respect to σ_h, respectively. In conclusion, $\psi_1\psi_2$ and $\psi_3\psi_4$ have components of ${}_\pi A_0^+$ and ${}_\pi A_0^-$ symmetry. Quite analogously, $\psi_1\psi_3$ and $\psi_2\psi_4$ contribute to ${}_0B_2^+$ and ${}_0A_2^+$, $\psi_1\psi_4$ and $\psi_2\psi_3$ to ${}_0A_0^+$ and ${}_0B_0^-$, and $\psi_1\psi_1$, $\psi_2\psi_2$, $\psi_3\psi_3$, and $\psi_4\psi_4$ to ${}_\pi A_2^+$, ${}_\pi A_2^-$, ${}_\pi B_2^+$, and ${}_\pi B_2^-$. Thus the symmetries of displacements, for which the integral (24) can be nonzero, are determined; the actual active modes are easily found by inspection, and they are specified in Table I. As far as the symmetry breaking is concerned, they form three classes:

(i) ${}_0Q_3$, and ${}_0Q_4$, which reduce the line group onto $\underline{L}_Q=\underline{L}/2mmm$,

(ii) ${}_\pi Q_1$ and ${}_\pi Q_2$, for which $\underline{L}_Q=\underline{L}'4/mmm$, and

(iii) ${}_\pi Q_3$, ${}_\pi Q_4$ and ${}_\pi Q_5$, with $\underline{L}_Q=\underline{L}'4_2/mcm$.

(The prime on $\underline{L}$ again indicates that the new translation period is $a'=2a$.)

Now, utilizing the results of Secs. III G, and IV C, one finds the band shapes of the distorted polymer, for each active mode Q. Thus after a distortion of the type (i), the band structure consists of four single lines (as in Sec. VI B); in case (ii) it contains four single lines and two double lines (as in Sec. VI A), while in case (iii) it consists of two double lines and two semiloops (each band folds at $k=\pi/2a$, but a gap opens only in the E band). In each of these cases, the degeneracy of the total electronic energy is completely lifted. (This need not be the case in general; a counterexample is given later in this section.)

Hence, this example has also brought in some novel features, the first of which is that several qualitatively different types of symmetry breaking are possible. Out of them, only the type-(ii) instabilities are similar to those studied in Secs. VI A and VI B. Namely, in that case the structure undergoes a periodic distortion, either by "dimerization" (as in the Peierls mode) or by alternating extension or contraction (as in the Feinberg-Ranninger mode). In contrast, the point-group symmetry of individual molecules is broken in a type-(i) distortion; this is similar to the classical Jahn-Teller effect. The difference is that here an extended chain is built out of such molecules, each of which distorts in the same way. Finally, type-(iii) instabilities are also new and very specific: The point-group symmetry of individual molecules is also broken, but some symmetry elements, such as, e.g., $(C_4 \mid 1)$, are restored through the staggered arrangement.

A similar analysis of the case when the E band of model IV, given by Eq. (30), is one-half-filled, also brings about a few surprises. First, the "Peierls" mode ${}_0Q_2$ is *not* active in this case. Next, the libration mode ${}_0Q_3$ [see Fig. 9(b)] is active here, but the total electronic energy remains degenerate after such distortion. Namely, in this case $\underline{L}_Q=\underline{L}2/mcc$, so that the band structure consists of two semiloops (see Sec. V B). The electronic degeneracy is just reduced, from fourfold to twofold, and the structure remains further unstable—with respect to the Peierls mode ${}_0Q_2$ and the Feinberg-Ranninger mode ${}_0Q_1$, as in Sec. VI B! This clearly illustrates the importance of investigating the band shapes of the polymer in distorted configurations for each active mode Q.

Many other interesting examples of vibronic instabilities can be found in Q1D crystals—e.g., the active modes

TABLE I. Active vibration modes of the polymer illustrated in Fig. 8(a), in the case when the doubly degenerate E band, given by (27), is one-half-filled. For the geometry of these modes see Fig. 8(b); the neighboring square molecules vibrate in-phase in the ${}_0Q_2$ and ${}_0Q_4$ modes, and out-of-phase in the remaining five modes. The symmetry labels ${}_\pi A_0^+$, ${}_0A_2^+$, etc., are explained in Sec. III C. AFDP is antiferrodisplacive, (A)FDT is (anti)ferrodistortive, TO is transverse optical, LA is longitudinal acoustic, and LO is longitudinal optical.

Mode	${}_\pi Q_1$	${}_\pi Q_2$	${}_0Q_3$	${}_\pi Q_3$	${}_0Q_4$	${}_\pi Q_4$	${}_\pi Q_5$
Symmetry	${}_\pi A_0^+$	${}_\pi A_0^-$	${}_0A_2^+$	${}_\pi A_2^+$	${}_0B_2^+$	${}_\pi B_2^+$	${}_\pi A_2^-$
Type	TO,AFDT	LA,AFDP	TO,FDT	TO,AFDT	TO,FDT	TO,AFDT	LO,AFDT

can be degenerate themselves [this happens in model IV if the A_0 band, as given by (28), is one-half-filled]; bands can overlap so that two or more pairs $\{k_F, -k_F\}$ are involved; then, there are other fillings and other band shapes to be considered. All these possibilities cannot be investigated here; the same is true for some important related questions (concerning the stable configurations, charge-density waves, excitation spectra, structural phase transitions, etc.) that go beyond the symmetry analysis.

VII. CONCLUSIONS AND DISCUSSION

Although lateral extension of typical polymers and quasi one-dimensional systems is relatively very small, band structures of such Q1D objects can differ essentially from those of proper 1D models. First, in the 1D case there is no band degeneracy, i.e., there are no two eigenstates $|k,\lambda\rangle$ and $|k,\lambda'\rangle$ such that $\epsilon_\lambda(k)=\epsilon_{\lambda'}(k)$. In contrast, in Q1D systems one frequently encounters twofold and even fourfold band degeneracies: Bands may intersect and/or may be degenerate throughout the BZ. Next, bands arising from a 1D periodic potential always have zero slope at $k=0$ and π/a, and they are monotonic functions of k in between.[4] In the Q1D case, crossings at $k=0$ and π/a enable the bands to have nonzero slopes at these points; on the other hand, closed shapes (such as loops, butterflies, etc.) may occur, in which case extrema are located somewhere inside the interval $(0,\pi/a)$.

The origin of these differences is that a Q1D model possesses the additional degrees of freedom, so that it may exhibit additional spatial symmetries, which in turn give rise to new quantum numbers. Together with the quasimomentum k, one has the quasi angular momentum m (arising from either a rotation-axis or a screw-axis symmetry) and also parities with respect to σ_v, σ_h, U, U_d, or S_{2n}. These quantum numbers essentially determine the band "shapes," i.e., their connectivity, degeneracy, location of crossings, and extrema, etc.

To be more specific, we have shown that in addition to single lines, for certain polymers, loops and double lines also appear in the JZ; its width is $n'2\pi/a$, and it is determined by the smallest fractional translation $(1/n')a\vec{e}_z$ appearing in the line group of the polymer considered.

Namely, lines with opposite momenta thread and form loops if the polymer is invariant with respect to $\underline{C}_n$ with $n \geq 3$; if mirror or glide planes are also present, these loops reduce onto $\{m,-m\}$ double lines. Transition to the more usual, BZ representation of the band structure, is made easily. In the absence of nonsymmorphic elements (i.e., glide planes or screw axes), $n'=1$ and the JZ coincides with the BZ. If $n'>1$, one simply folds the entire figure n' times; in this way, more complex shapes (e.g., double semiloops, butterflies, etc.) can be obtained. Screw axes of arbitrarily large order are possible in principle (although there certainly are experimental resolution limits), and in this sense the number of topologically inequivalent possible band shapes in the BZ is unlimited.

Thus an explicit relationship has been established between some structural characteristics of a polymer and certain qualitative features of its band structure and the density-of-states function. This may provide useful guidelines in the search for a polymer with specific electronic properties. Another application would be to check calculated band structures; notice that finite-size basis sets are utilized in such computations and one predicts not only the possible band shapes, but also how many times a given shape occurs. (These numbers depend on the atomic positions—more precisely, only whether the atoms lie in symmetry lines or planes is important—and on the type of the basis functions.) Finally, the band interpolation problem is resolved.

The information about the number of DOS peaks and the quantum numbers that characterize them, combined with the selection rules for different processes, is useful for interpreting experimental data—in structural analysis, for assignment of the observed transitions, in studies of structural phase transitions, and the effects of the crystal and external fields. Notice that the magnetic field removes the time-reversal invariance, so that the band structure may lose its symmetry with respect to the $k=0$ axis; this cannot happen if the line group contains $(\sigma_h \mid 0)$, $(U \mid 0)$, $(U_d \mid 0)$, or $(S_{2n} \mid 0)$, since these elements revert the quasimomentum.

As another application, the above results on band shapes and the quantum numbers that characterize them provide a powerful, yet simple method for symmetry analysis of vibronic coupling in Q1D solids. In each case, one can proceed as follows: (a) Determine the line group $\underline{L}$ of the polymer considered, (b) find the band shapes, (c) read the quantum numbers (k_F, m_F, etc.) of the degenerate electronic states at ϵ_F, (d) determine from them the active modes Q; then, for each Q, (e) find the reduced line group $\underline{L}_Q$ and (f) the corresponding band shapes, and (g) check whether the electronic degeneracy is completely lifted, or not. Several examples are analyzed along these lines in the present paper, and the results display another important consequence of the fact that band structures of polymers may contain complex band shapes: Vibronic instabilities of various types can appear in the case when the total electronic energy is degenerate. Indeed, the phonons involved may be acoustic or optical, longitudinal or transversal, etc.; also, different types of symmetry breaking are possible.

Finally, although our attention has been focused on band structures of polymers, the results of this paper are equally applicable to dispersion curves of other quasiparticles (e.g., phonons) for which the effective Hamiltonian commutes with the line group of the polymer. They are even valid for systems of higher dimensionalities, as long as one studies the $\epsilon_\lambda(\vec{k})$ functions with $\vec{k}$ varying along a specified (high-symmetry) direction in the reciprocal space.

ACKNOWLEDGMENTS

The clarity of presentation of this paper owes much to numerous suggestions of Professor Leo Falicov. Hospitality of the Department of Physics, University of California, Berkeley is also gratefully acknowledged, as well as the financial support from the Council for International Exchange of Scholars (a Fulbright award) and the National Science Foundation Grant No. DMR-81-06494.

*Present and permanent address: Institute of Physics, P.O. Box 57, 11001 Belgrade, Yugoslavia.

[1]*Extended Linear Chain Compounds,* edited by J. Miller, (Plenum, New York, 1982), Vols. 1—4; Proceedings of the International Conference on Low-Dimensional Conductors, Boulder, Colorado, 1981, edited by A. J. Epstein and E. M. Conwell, [Mol. Cryst. Liq. Cryst. 77, (1981); 79, 81, 83, 85, 86, (1982)]. D. Jérome and H. J. Schultz, Adv. Phys. 31, 299 (1982), and references therein.

[2]J.-M. André, Adv. Quantum Chem. 12, 65 (1982).

[3]L. Van Hove, Phys. Rev. 89, 1189 (1953); J. C. Phillips, *ibid.* 104, 1263 (1956); E. I. Rashba, Fiz. Tverd. Tela (Leningrad) 1, 407 (1959) [Sov. Phys. Solid State 1, 368 (1959)]; V. I. Sheka, *ibid.* 2, 1121 (1960) [2, 1096 (1960)]; G. F. Karavaev, *ibid.* 6, 3676 (1964) [6, 2943 (1965)]; N. V. Kudryavceva, *ibid.* 9, 2364 (1967) [9, 1850 (1968)]; 10, 1616 (1968) [10, 1280 (1968)]; J. Killingbeck, Rep. Prog. Phys. 33, 533 (1970).

[4]W. L. McCubbin and F. A. Teemull, Phys. Rev. A 6, 2478 (1972).

[5]M. Lax, *Symmetry Principles in Solid State and Molecular Physics* (Wiley, New York, 1974).

[6]C. Hermann, Z. Kristallogr. 69, 250 (1928); E.Alexander, *ibid.* 70, 367 (1929); B. K. Vainshtein, *Diffraction of X-Rays by Chain Molecules* (Elsevier, Amsterdam, 1966), p. 53; M. Vujičić, I. Božović, and F. Herbut, J. Phys. A 10, 1271 (1977).

[7]I. Božović, M. Vujičić, and F. Herbut, J. Phys. A 11, 2133 (1978); I. Božović and M. Vujičić, *ibid.* 14, 777 (1981); I. Božović and N. Božović, *ibid.* 14, 1825 (1981).

[8]I. Božović, J. Delhalle, and M. Damnjanović, Int. J. Quantum Chem. 20, 1143 (1981); M. Damnjanović, I. Božović, and N. Božović, J. Phys. A 16, 3937 (1983); *ibid.* (in press).

[9]L. P. Bouckaert, R. Smoluchowski, and E. Wigner, Phys. Rev. 50, 58 (1936); S. L. Altmann and C. J. Bradley, Rev. Mod. Phys. 37, 33 (1965).

[10]B. Wunderlich, *Macromolecular Physics* (Academic, New York, 1973), Vols. 1 and 2; A. I. Kitaigorodski, *Molecular Crystals and Molecules* (Academic, New York, 1973); R. L. Miller, in *Polymer Handbook,* 2nd ed., edited by J. Brandrüp and E. H. Immergut (Wiley, New York, 1975), Part III, p. 1.

[11]I. Božović and J. Delhalle, Phys. Rev. B 29, 4733 (1983).

[12]M. Tinkham, *Group Theory in Quantum Mechanics* (McGraw-Hill, New York, 1964).

[13]J. von Neumann and E. Wigner, Phys. Z 30, 467 (1927) [English translation in R. S. Knox and A. Gold, *Symmetry in the Solid State* (Benjamin, New York, 1965), p. 157]; E. Teller, J. Phys. Chem 41, 109 (1937); R. K. Nagvi and W. Byers Brown, Int. J. Quantum Chem. 6, 271 (1972); R. K. Nagvi, Chem. Phys. Lett. 15, 634 (1972).

[14]A. Blumen and C. Merkel, Phys. Status Solidi B 83, 425 (1977); J. Ladik, in *Excited States in Quantum Chemistry,* edited by C. A. Nicolaides and D. R. Beck (Reidel, Dordrecht, 1978), p. 495.

[15]M. Sachs, *Solid State Theory* (McGraw-Hill, New York, 1963); R. Bube, *Electrons in Solids* (Academic, New York, 1981).

[16]H. A. Jahn and E. Teller, Proc. R. Soc. London, Ser. A 161, 220 (1937).

[17]R. E. Peierls, *Quantum Theory of Solids* (Oxford University Press, London, 1955).

[18]D. Feinberg and J. Ranninger, J. Phys. C 16, 1875 (1983).

[19]In the traditional approach one has to construct and to reduce $[D^2]$, which in the case considered is a ten-dimensional representation of an infinite group—a tedious task in practice.